Spectroscopic Studies on the Interaction of Tetramethylpyridylporphyrins and Cationic Clays

PATRÍCIA M. DIAS, DALVA L. A. DE FARIA and VERA R. L.
CONSTANTINO⋆
*Instituto de Química, Universidade de São Paulo, Caixa Postal 26 077, CEP 05513-970, São Paulo,
SP – Brazil*

Abstract. In the present work, the interaction between 5,10,15,20-tetrakis(1-methyl-4-pyridyl)-21*H*,23*H*-porphine (TMPyP) and its metallated form (CoTMPyP) with three cationic clays was investigated by X-ray diffraction (XRD), UV-VIS and resonance Raman spectroscopies. Sodium montmorillonites K10 and KSF and a synthetic fluorohectorite (FHT) containing different macrocycle loadings, were prepared by an ion exchange reaction. In nonsaturated KSF and FHT, the CoTMPyP molecule assumes a flat orientation, relative to the host layers, giving rise to at least two absorption bands in the Soret region (ca. 445 and 465 nm) assigned to adsorbed and intercalated CoTMPyP, respectively. For the delaminated K10 sample, a broad band centered around 456 nm, indicates a major contribution from the metalloporphyrin on the clay external surfaces. The electronic spectra of FHT samples containing increasing amounts of CoTMPyP show bands red shifted even when a small amount of porphyrin is used, suggesting that the electronic levels of the macrocycle are more affected by the interaction with the clay than by the metalloporphyrin distortion inside the galleries. The resonance Raman spectra obtained for all CoTMPyP samples presented only minor shifts in peak positions and band width, with the exception of the FHT saturated sample, where the bands are clearly broader when compared to other loadings, suggesting that porphyrin aggregation is occurring. In the case of TMPyP, the bands at ca. 430 and 468 nm were assigned to nonprotonated and protonated molecules, respectively. This assignment is supported by resonance Raman spectroscopy, which also showed the ν_2 mode (ca. 1550 cm^{-1}) to be the most sensitive peak to protonation.

Key words: smectite, cationic clays, porphyrins, metalloporphyrins, intercalation compounds, Raman spectroscopy.

1. Introduction

Some layered compounds show intracrystalline reactivity, i.e., neutral and/or charged species can be incorporated in the interlayer space under mild conditions [1]. Taking into account the intercalation chemistry field, one of the most explored systems comprises the layered silicates of the smectite group. The swelling and ion exchange properties of smectite clays are well known and explored in academic and technological institutes [1–5]. Currently, widespread research has been performed,


⋆ Author for correspondence.

aimed at the structural modification of these cationic clays for applications as molecular sieve and shape selective catalysts for organic molecules [2–4].

The smectite clay structure consists of a central sheet of $MO_4(OH)_2$ octahedra symmetrically bonded to two MO_4 tetrahedral sheets (T : O : T layers, Figure 1a). The octahedral sites are occupied by ions like aluminum, magnesium and iron, while the tetrahedral centers accommodate silicon and aluminum ions. The negative lamellae charge arises from isomorphic ion substitutions and it is neutralized by the presence of hydrated cationic ions between the layers [5].

Among several species employed in clay intercalation studies are the porphyrins, which are macrocyclic molecules containing a highly conjugated ring system made up of four pyrrole units linked by four methine bridging groups (Figure 1b), and are responsible for some very important biological processes [6]. Their occurrence in oil deposits and sediments stimulated the former works on the porphyrin adsorption processes in clays considering the geological environment [7, 8]. Subsequent studies were aimed at the characterization of different kinds of natural clays intercalated with neutral and non-metallated porphyrins [9, 10], as well as several metallated derivatives [11]. The literature has also reported the insertion of cationic species as free base [12, 13] and metallated species [12, 14–16]. In these articles, the macrocycle orientation in the interlayer region and some possible reactions, such as metallation and protonation (free base) or demetallation (metalloporphyrins), as well as changes in the molecular electronic configuration, have been investigated mainly by X-ray diffraction and UV-VIS spectroscopy (absorption and diffuse reflectance). Additional techniques such as infrared vibrational spectroscopy [9, 10], electron paramagnetic resonance (EPR) [15, 16], thermal analysis [17] and X-ray photoelectron spectroscopy (XPS) [18] have also been used. The characterization of macrocycle-smectite systems obtained using TMPyP and TMAP as templates for the synthesis of hectorite was also reported [19].

The attention generated by intercalated layered systems can be attributed mainly to the fact that chemical and physical properties of host and guest are often significantly changed by the interaction. Concerning the occurrence of selective chemical reactions in the intracrystalline space containing reactive guest species, there are reports on the intercalation of synthetic models such as metallated porphyrins, phthalocyanines and Schiff bases that mimic natural enzymatic systems [20, 21]. Cationic clays containing metalloporphyrins have also been evaluated as catalysts for alkene epoxidation and alkane hydroxylation [22], reductive dehalogenation [23] and phenol oxidation [24].

Vibrational spectroscopy (IR and Raman) is one of the most employed spectroscopic techniques to probe molecular interactions and environment conditions. Concerning the porphyrin-clay system, resonance Raman spectroscopy [25] seems to be the technique of choice, as the spectrum is free from matrix interference as the smectites besides being poor light scatterers do not absorb in the visible.
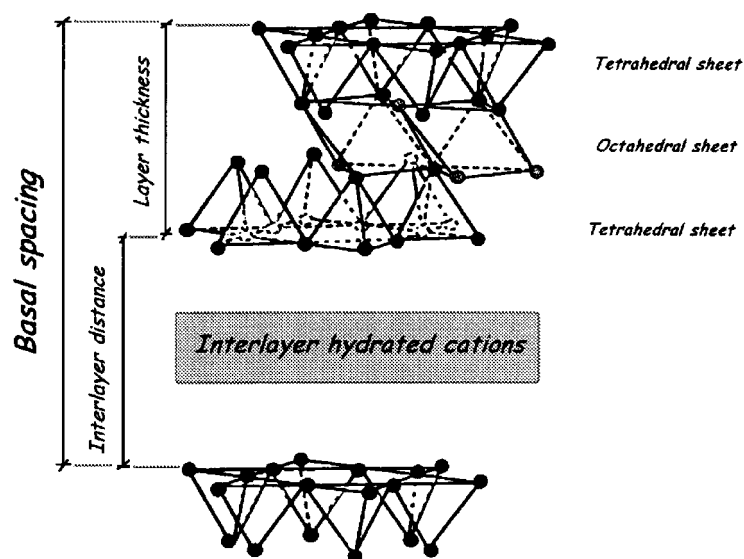
(a)
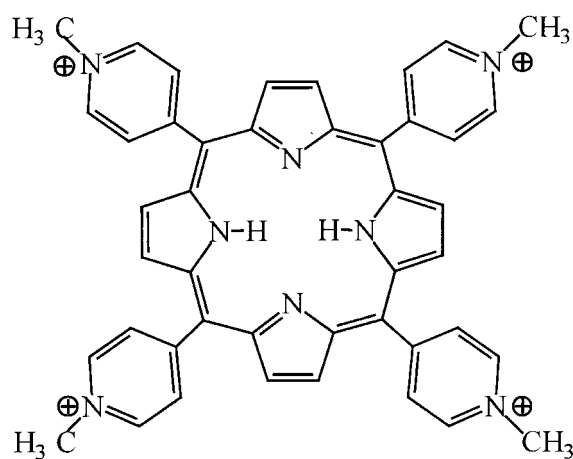
(b)

Figure 1. Schematic representation of (a) a 2 : 1 layered silicate and (b) a *meso*-substituted porphyrin (TMPyP).

Despite the sensitivity provided by the resonance Raman technique to distortions in symmetry [26, 27], perturbation in electronic distribution [28] and environmental properties [29], very few attempts were made to employ it in the characterization of porphyrin intercalates in inorganic matrices [30–32], or even intercalates with other organic molecules [33–36].

There are some disagreements in the literature concerning the changes observed in the electronic absorption spectra (bathochromic shift) when TMPyP interacts with clays. Some authors [9, 10, 12, 37] found evidence that *meso*-substituted free base porphyrins are protonated by the acidic sites on the clay surface while others support the idea of TMPyP flattening caused exclusively by a rotation of the methylpyridyl group around the C_m-C_{MePy} bond [38] and not to protonation. Resonance Raman spectroscopy is the technique of choice to address these questions as it has proved to be sensitive to protonation [39] and structural distortions [40–42].

In the present work the interaction between the macrocycles TMPyP and CoT-MPyP and three cationic clays was investigated by electronic spectroscopy and, for the first time, by resonance Raman spectroscopy. The degree of layer stacking and the charge density of the clays as well as the macrocycle arrangement relatively to their layers were considered.

2. Experimental

2.1. MATERIALS AND METHODS

Commercial clay montmorillonite KSF (Aldrich, surface area: 20–40 m^2/g) and acid treated clay montmorillonite K10 (Aldrich, surface area: 220–270 m^2/g) were exchanged to the sodium form by employing NaCl solution (5 mol/L), and washed by centrifugation with deionized water as described in the literature [22]. Synthetic clay fluorohectorite (abbreviated FHT, from Corning) was used without previous treatment. Free-base 5,10,15,20-tetrakis(1-methyl-4-pyridyl)-21*H*,23*H*-porphine (TMPyP, chloride salt, Mid-Century) and the metallated form (CoTMPyP, chloride salt, Mid-Century) were used as received.

The cation exchange capacity (CEC) of the sodium clays K10 (K10-Na) and KSF (KSF-Na), and FHT was evaluated according to a spectrophotometric method suggested in the literature [43] employing [Co(NH$_3$)$_6$]Cl$_3$. The cobalt complex was prepared as described previously [44] and characterized by elemental analysis and UV-VIS spectroscopy.

The CEC of K10 (26 meq/100 g) is inferior to that obtained for KSF (62 meq/100 g) and the structure is another parameter that can distinguish these two montmorillonite clays: K10 has a delaminated structure which is verified by the absence of 00l X-ray reflections [45, 46] and a higher surface area when compared to KSF. The "face-to-face" K10 aggregation involves only a few layers and XRD patterns for the sodium form revealed only the presence of diffraction peaks that can be attributed to mica (d = 9.9, 4.9 and 3.3 Å) [47]; the same impurity was also identified in KSF together with the 00l reflections (d_{001} = 13.10 Å). The basal reflection for FHT is 12.07 Å and its CEC is very high (192 meq/100 g).

K10, KSF and FHT containing different porphyrins loadings were prepared, adding aliquots of the silicate matrices to the macrocycle aqueous solution. The suspensions were maintained under reflux and heating at 60–70 °C for ca. 40 h. The

solids were isolated and washed with deionized water by centrifugation or dialysis. Saturated samples (prepared from solutions containing an excess of porphyrin relative to the clay CEC) were washed until a clear supernatant was obtained. Nonsaturated samples produced a clear supernatant and the washing step did not remove the macrocycle from the clay particles. The samples were dried with P_4O_{10} in an Abderhalden apparatus or in a evacuated desiccator. The slides of oriented samples for XRD analysis were prepared by drying an aqueous and diluted clay suspension over a glass disk in a desiccator with silica gel. Unless otherwise stated, the percentage amounts of the macrocycles in the clays refers to CEC.

2.2. EQUIPMENT

XRD patterns of oriented films were recorded on a Philips diffractometer model PW1710, using CuK_α radiation ($2\theta = 2.5$–$45°$). UV-VIS absorption spectra of aqueous solutions were recorded with a Hitachi model U-2000 spectrophotometer. A Shimadzu model UV-2401PC spectrophotometer, equipped with an integration sphere, was employed to record the diffuse reflectance spectra. $BaSO_4$ (Waco Pure Chem.) was used to dilute the samples. Resonance Raman spectra were obtained using a Renishaw Raman System (model 3000) fitted with a Peltier cooled CCD detector (Wright, 600×400 pixels) and a metallurgical microscope (Olympus). The spectra were excited at 457.9 nm, by an air cooled Ar^+ laser (Omnichrome) and the samples were investigated on glass slides by a $\times 80$ lens with the laser power kept at 70 μW to avoid thermal degradation.

3. Results and Discussion

3.1. CHARACTERIZATION OF THE PORPHYRIN-CLAY SYSTEMS

The three smectite clays used in the present work have isomorphous substitution in the octahedral centers [4]. In montmorillonite, Al^{3+} ions are replaced partially by Mg^{2+} and, to a lesser extent, by Fe^{3+}; the Si^{4+} can be replaced by Al^{3+} in the tetrahedral interstices. Considering FHT, a synthetic hectorite, the Mg^{2+} ions are partially substituted by Li^+, which is also present between the layers as exchangeable cation, and the hydroxide groups of octahedral sheets are substituted by fluorine.

Figure 2 shows the XRD patterns of FHT containing increasing amounts of CoTMPyP. If the thickness of the T:O:T layer (9.6 Å) [5] is subtracted from the basal spacing, the gallery height can be estimated as 9.1, 6.1 and 4.1 Å for samples containing 100, 50 and 10% of CoTMPyP, respectively. In the case of the saturated sample (100% of CEC), a similar result is reported in the literature ($d_{001} = 18.6$ Å or gallery height of 9 Å) [24] and was attributed to an inclined arrangement of the porphyrin ring relative to the silicate layers. Taking into account the TMPyP dimensions (ca. 17.5 Å $\times$ 17.5 Å $\times$ 4 Å [15, 48]), we can attribute the basal spacing observed for the 50% sample to a monolayer of hydrated CoTMPyP intercalated in
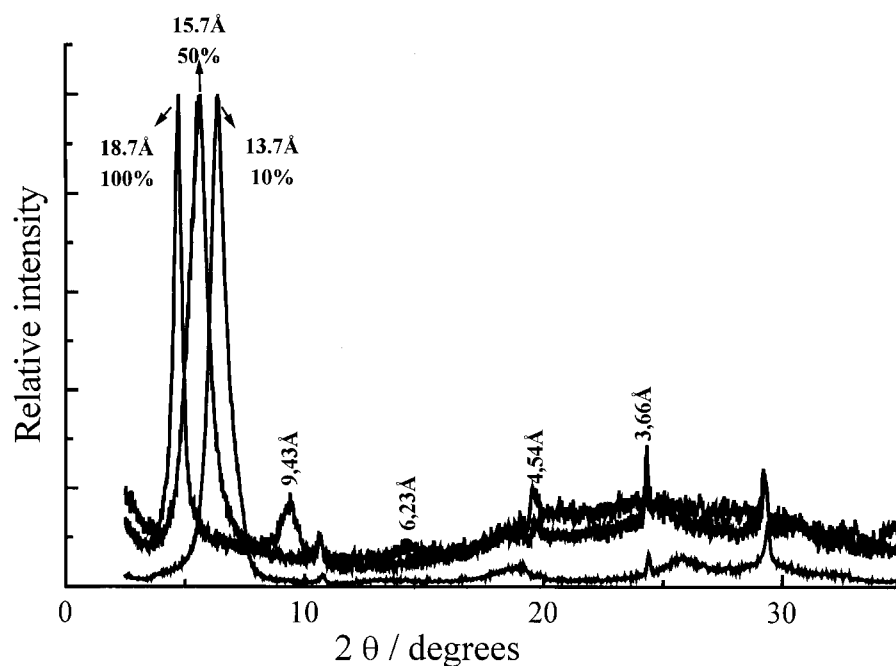
Figure 2. XRD patterns of FHT samples containing 10, 50 and 100% of CoTMPyP.

a flat orientation or tilted by 27° relative to the lamellae. This point will be further discussed. At low CoTMPyP loading (about 10%), the observed basal spacing is in agreement with previously reported data [14], suggesting that the macrocycle is within the interlayer space. Another explanation is that CoTMPyP is on the external surface and the interlayer space is occupied by Li^+ with a higher degree of hydration than in the FHT precursor. Actually, it is not possible to determine by XRD if the guest species is intercalated or not when the macrocycle amount is very small.

The XRD pattern recorded for KSF containing 13% of CoTMPyP showed a basal spacing decrease from 13.1 Å to 12.8 Å (XRD not shown). A lower interlayer height was also observed in the literature for a montmorillonite treated with a small amount of CoTMPyP [14]. The presence of CoTMPyP in the K10 sample does not change the XRD pattern observed for this clay in the Na^+ form, evidencing the absence of long-range stacking.

For TMPyP saturated samples, the XRD data showed a d_{001} value of 18.9 and 14.7 Å for FHT and KSF, respectively (XRD not shown). The difference in the interlayer height can be interpreted in terms of the layer charge densities of the smectites. The montmorillonite KSF has a lower charge density than FHT, favoring a flat orientation of the porphyrin relative to the layers. When intercalated in FHT, TMPyP takes a tilted position between the layers as observed for the same clay saturated with CoTMPyP. K10 samples with 13 and 100% of TMPyP were
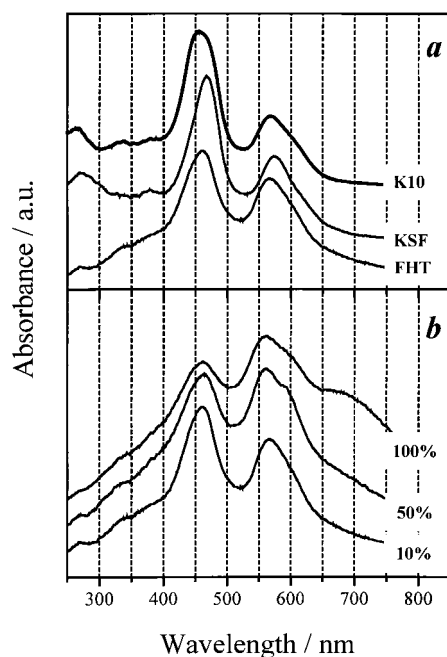
Figure 3. Diffuse reflectance spectra of nonsaturated clays with CoTMPyP: (a)K10, KSF and FHT (10%). (b)FHT clay containing increasing CoTMPyP loadings.

prepared and the XRD peaks relative to the layer stacking were also not observed as in the case of CoTMPyP.

3.2. ELECTRONIC SPECTROSCOPY DATA

Porphyrins present a very characteristic UV-VIS spectrum, dominated by $\pi \rightarrow \pi^*$ transitions (Soret and Q bands) located at ca. 400 nm and 550 nm, respectively [49]. Figure 3a shows the diffuse reflectance spectra of K10, KSF and FHT clays containing CoTMPyP (non-saturated samples). As can be observed, the Soret and Q bands are red shifted after CoTMPyP interaction with the clays when compared to the free metalloporphyrin (Table I).

This bathochromic shift has been observed for solid samples [11, 12] and water suspensions [10, 11, 14, 16] containing clays and metalloporphyrins. For CoT-MPyP systems in particular, visible absorption data were reported for the solids in suspension. It was verified that for hectorite, containing different CoTMPyP loadings (10, 50 and 100%) and in a flat orientation, the spectra show a shoulder at ca. 440 nm and bands at 468 and 574 nm [16]. In a work with saponite clay [14], a band at 450 nm was attributed to the CoTMPyP adsorbed on the external surface of silicate sheets, while the peak at 465 nm was assigned to the intercalated metalloporphyrin. Figure 3a shows the presence of at least two bands in the Soret region for the clay samples containing CoTMPyP. From the above cited works, we can

Table I. Electronic spectroscopy data for CoTMPyP and TMPyP-clay samples.

Sample	Absorption maxima (λ/nm) [a]
CoTMPyP [b]	444 (S); 558; 607, 695; ca. 785 (br)
K10 – CoTMPyP (34%)	456 (S, br), 465 (sh); 567, 600 (sh)
KSF – CoTMPyP (13%)	ca. 445 (sh), 467 (S); 573, 610 (sh)
FHT – CoTMPyP (10%)	ca. 445(sh), 460 (S), 566, 600 (sh)
FHT – CoTMPyP (50%)	450 (sh), 463 (S); 561; 594 (sh)
FHT – CoTMPyP (100%)	450 (sh), 462 (S); 560, 595 (sh), ca. 680 (br)
TMPyP [b]	424 (S); 522; 559 (sh); 600; 661
TMPyP (pH = 1) [b]	455 (S), 600, 652
KSF – TMPyP (100%)	428 (sh), 472 (S), 583 (sh), 619, 672 (sh)
FHT – TMPyP (100%)	430 (sh), 468 (S); 542; 596; 654
K10 – TMPyP (100%)	426 (sh), 465 (S), 552 (sh), 593; 614 (sh), 674 (sh)
K10 – TMPyP (13%)	463 (S), 540 (sh), 585 (sh), 613, 673

[a] (S), (sh) indicate the Soret band and a shoulder, respectively; (br) means broad.
[b] Data recorded for the compounds in the solid state. Protonated TMPyP was obtained through the evaporation of a HCl solution (pH = 1) containing the macrocycle.

infer that in K10, the CoTMPyP molecules are located mainly at the external basal surface, while for KSF and FHT, the majority of macrocycle ions is intercalated between the layers. This interpretation seems plausible, since K10 is a delaminated clay (house-of-cards structure) and only a few layers are aggregated "face-to-face". Comparing the spectra of KSF and FHT (Figure 3a), one can assume that the amount of intercalated CoTMPyP is higher in the former clay, an expected result if we consider that the layer charge density of KSF is lower than the FHT one, facilitating the intercalation process. In the Q bands region, only two peaks are observed, which indicates that the D_{4h} macrocycle symmetry is maintained after the interaction with the clay surfaces.

The diffuse reflectance spectra of FHT containing increasing amounts of CoTMPyP is shown in Figure 3b. In all cases, the Soret band was observed at ca. 462 nm whilst the Q bands present a larger red shift when a small amount of porphyrin is used (566 nm for 10% loading and 560 nm for the other ones). When compared with the data for the free porphyrin (444 and 558 nm), the UV-VIS spectrum suggests that the electronic levels of the macrocycle are affected by the interaction, but not by the metalloporphyrin orientation in the gallery region. Figure 3b also reveals a substantial decrease in the intensity of the Soret band, relative to the Q bands, when the CoTMPyP loading is close to the saturation condition. The same behavior was observed for a sodium montmorillonite after reaction with MTPP (M = Mg^{2+} and Zn^{2+}) and was attributed to the presence of porphyrin aggregates at the silicate surface [11]. The presence of a broad band at ca. 680 nm in the
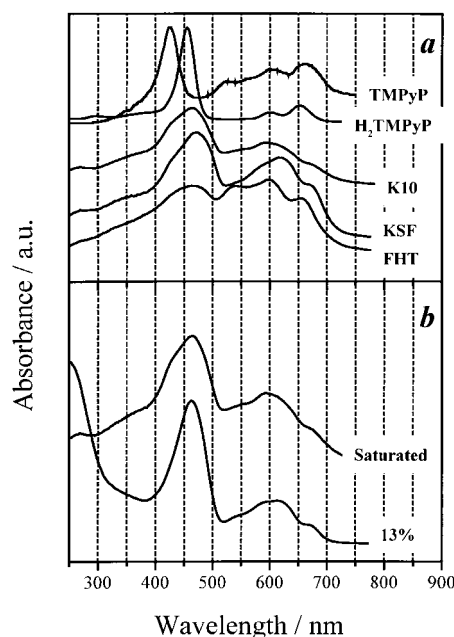
Figure 4. Diffuse reflectance spectra of (a) TMPyP, H_2TMPyP and the K10, KSF and FHT clays saturated with TMPyP; (b) K10 containing 13% and 100% of TMPyP.

saturated sample is characteristic of porphyrin aggregates [50] and confirms such a supposition.

Smectite clays usually interact with free base porphyrins generating green solids which has been explained as arising from porphyrin protonation [10, 12]. Water molecules coordinated to exchangeable metal cations or to undercoordinated metal atoms on the broken-edges are responsible for the Brönsted acidity of clay minerals [51]. Figure 4a shows the electronic spectra of K10, KSF and FHT samples, saturated with TMPyP. The spectra of protonated and non-protonated TMPyP were included in the figure for comparison purposes. K10 and KSF samples are green while FHT is brown, which at first glance indicates that the later is less acidic than the montmorillonite samples. The Soret and Q bands of the clay samples spectra are red shifted, relative to the free base or its protonated form.

The spectra of the saturated samples clearly show two peaks around 450 nm. The higher energy one (ca. 430 nm) corresponds to the non-protonated porphyrin, while the band centered at ca. 465 nm can be assigned to the protonated TMPyP, leading to the conclusion that not all the porphyrin molecules are protonated. An inspection in the region of the Q bands confirms this hypothesis and suggests that the TMPyP is less protonated in FHT than in K10 and KSF. Comparing the spectra of the montmorillonite samples, it can be observed that the bathochromic shift of Soret and Q bands is the largest in KSF. This behavior can be due to the fact that in KSF the guest species are mainly confined between the layers, while in K10,

the macrocycle ions are on the external surface, as discussed previously, for the samples containing CoTMPyP. The low intensity of the Soret band when compared to the Q band, suggests that, in FHT samples saturated with TMPyP, the macrocycle is aggregated in the galleries.

Figure 4b shows the spectra of K10 containing two different amounts of TMPyP. At low loading, the band at 465 nm is very intense and indicates that almost all macrocycle species are protonated. When K10 is saturated with the porphyrin, the intensity of the band assigned to the non-protonated species increases substantially, indicating that the acidic sites available cannot protonate all the molecules. The intensity of the bands in the Soret region decreases when compared to the Q bands for the saturated sample, suggesting porphyrin aggregation, a process which may promote the stacking of K10 layers. The XRD pattern of K10 samples containing 50 and 100% of TMPyP (XRD not shown) presents a broad diffraction peak at 4.2–6.4° (2θ degrees) that can arise from the "face-to-face" assembling arrangement incorporating TMPyP dimers or eventually higher aggregates.

3.3. RESONANCE RAMAN SPECTROSCOPY

Besides protonation and distortions, the Raman spectra of the TMPyP-clay systems are likely to present some changes when compared to the free porphyrin, as a consequence of the geometry of interaction (parallel, perpendicular or tilted, relative to the host walls) and environmental conditions (electrical field, dielectric constant etc). Such effects are not exclusive and the Raman spectrum is very likely to contain contributions from some of them.

Figure 5 shows the Raman spectra of FHT, KSF and K10 saturated with TMPyP. Comparing these spectra with the TMPyP one, only minor changes were observed for FHT, in contrast to KSF and K10, which showed a significant shift in the ca. 1550 cm^{-1} peak position. Structure-sensitive Raman bands were identified as the ν_2, ν_3, ν_4 and ν_{19} modes [27], which in the TMPyP spectrum shows up at 1556, 1444, 1364 and 1600 cm^{-1}, respectively, in solution at pH 7 [39] (actually the peak at 1600 cm^{-1} is usually not observed in solution but appears as a weak band in the spectrum of the solid sample shown in Figure 5). Non-planar structures can also be detected from the wavelength dependence of the depolarization ratios [26] but, unfortunately, this information is not available for solid samples. In the case of K10 and KSF containing TMPyP, all the structure-sensitive vibrations are not affected, except the ν_2 mode, and it is not possible to conclude whether or not distortion is occurring from only the spectra shown in Figure 5.

In Figure 5, the spectrum of the diprotonated porphyrin (H$_2$TMPyP) is included for comparison purposes. Again, in spite of the shift in the ca. 1550 cm^{-1} band, there are other peaks that are also affected by protonation. This fact suggests two different explanations: (i) the porphyrin is only monoprotonated when interacting with the clays. The singly protonated species would give a different spectrum when compared to the doubly protonated one, which could account for the poor agree-
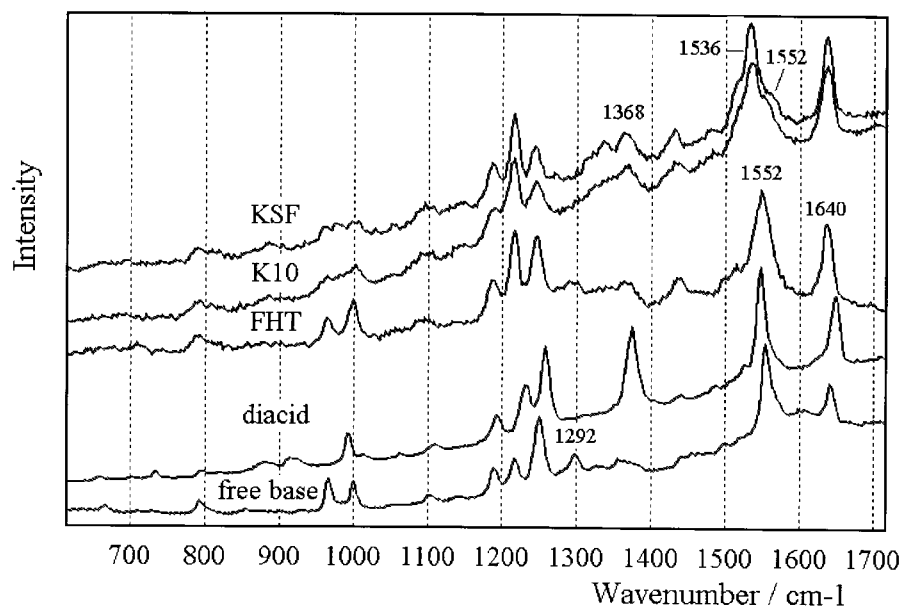
Figure 5. Resonance Raman spectra of TMPyP, H_2TMPyP and the K10, KSF and FHT clays saturated with TMPyP.

ment between the clay-TMPyP spectra in Figure 5 and the diacid spectrum. The monoprotonated form of TMPyP cannot be isolated [52], thus making it impossible to obtain a reference spectrum; (ii) both protonation and distortion are occurring, which together with the confinement effect, would promote only minor changes in the porphyrin spectrum.

At this point it is important to emphasize that when CoTMPyP interacts with the same clays, its Raman spectrum (Figure 6) is much less affected than in the case of TMPyP (1577, 1575 and 1575 cm^{-1} for FHT (50%), K10 and KSF samples containing CoTMPyP, respectively). Furthermore, all the samples are brown in color (so is the FHT sample saturated with TMPyP), despite some red shift and broadening of both Soret and Q bands in the UV-VIS spectra.

To clarify this point, K10 and FHT samples saturated with TMPyP were exposed to HCl vapors. The FHT sample acquired quickly a dark green color while the K10 one, which was already green, only had its color enhanced. The respective Raman spectra are shown in Figure 7, which also includes the spectra of samples before the acid treatment. As can be seen, the K10 spectrum remains unaltered after being exposed to HCl, whilst in the case of the FHT sample, the ν_2 mode shifts downwards. After acid treatment, the position of the ca. 1550 cm^{-1} band for TMPyP in FHT and K10 is exactly the same (1536 cm^{-1}), indicating that in K10 the porphyrin was already doubly protonated and that the ca. 1550 cm^{-1} peak is sensitive to protonation, not depending on the orientation within the interlayer region. It is also remarkable that even when doubly protonated (Figure 7), the Raman
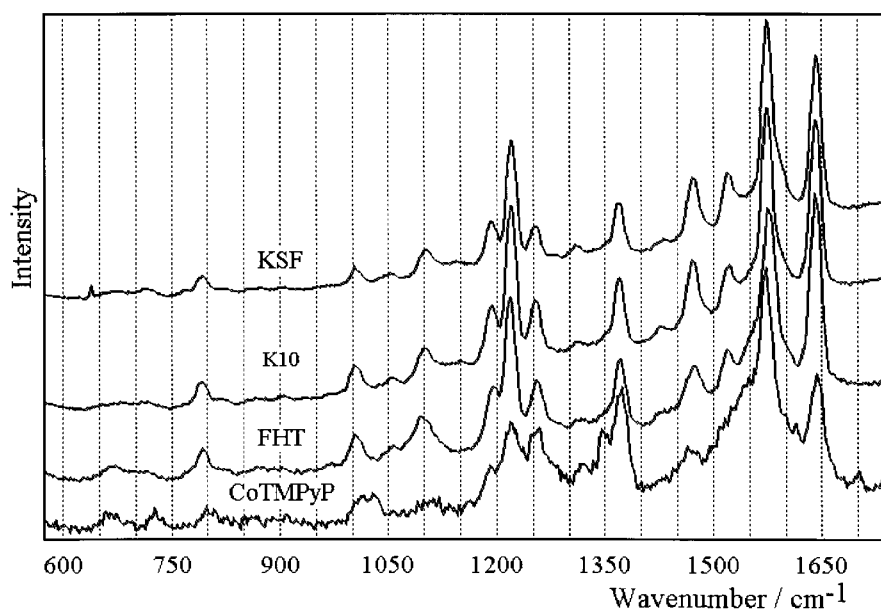
Figure 6. Resonance Raman spectra of CoTMPyP and K10, KSF and FHT clays with CoTMPyP (nonsaturated).

spectrum of the TMPyP intercalated in K10 is not similar to the free H_2TMPyP one (solid sample).

From the above arguments it follows that the 1555 cm^{-1} band shifts to 1535 cm^{-1} when TMPyP is doubly protonated on the clay surface. As some molecules are not protonated, their contribution to the spectra are shown in Figure 8, which presents the Raman spectrum of the K10 sample containing two different loadings. At 13% loading most molecules are protonated and the 1550 cm^{-1} peak appears as a weak shoulder of the strong 1536 cm^{-1} band. However, when the clay is saturated with TMPyP, the 1555 cm^{-1} band is much more prominent. Such an explanation is confirmed by diffuse reflectance spectroscopy (Figure 4b), which shows only the Soret band at 460 nm (intercalated diacid) for the 13% sample but a shoulder is clearly observed at 430 nm (free porphyrin) in the case of the saturated clay.

Summing up, the layer charge densities in K10 and KSF are considerably lower than in FHT, which makes the parallel orientation of the guest more likely to occur, as observed for other systems [10, 12, 16]. Since the diacid form is more distorted than the free base [53], some degree of porphyrin distortion is also expected in the K10 and KSF samples. However, the fact that the Raman spectra of the CoTMPyP samples are much less sensitive to intercalation than the TMPyP ones, clearly indicates that protonation and not distortion is exerting the strongest influence on the Raman spectra.
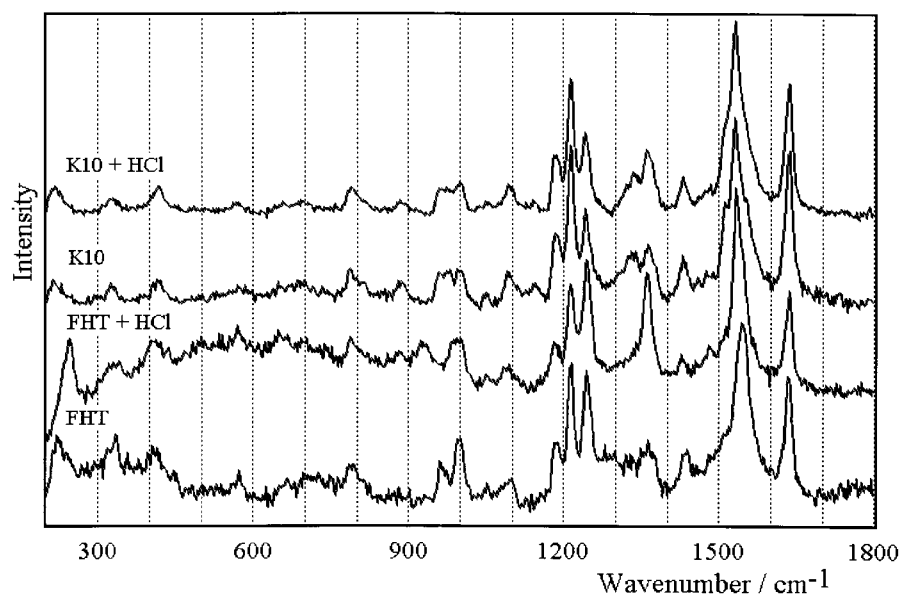
Figure 7. Resonance Raman spectra of K10 and FHT saturated with TMPyP after exposure to HCl vapors.
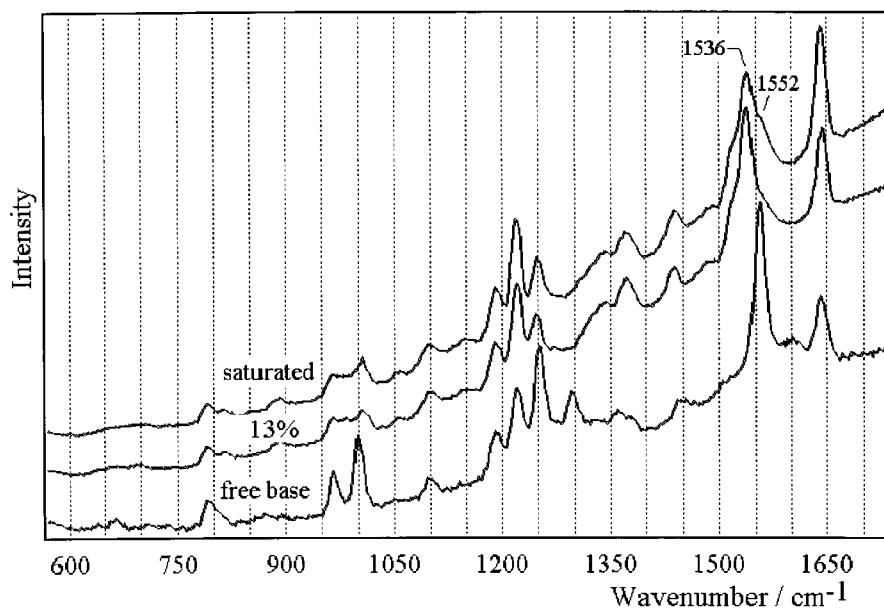

Figure 8. Resonance Raman spectra of K10 containing 13% and 100% of TMPyP. The free base spectrum is included for comparison purposes.

FHT samples containing 10, 50 and 100% of CoTMPyP were also studied. The Raman spectra (not shown) are not significantly affected by the macrocycle concentration, except in the case of the saturated sample in which the much broader bands suggest that porphyrin aggregation is occurring, in agreement with the interpretation given to the UV-VIS absorption data. Some authors have attributed the red shift in the Soret and Q bands, observed after interaction with clays, to a twist of the methylpyridyl substituent towards the porphine ring plane, leading to a more planar structure [38]. If this explanation was correct, the Raman spectrum of the FHT with low CoTMPyP concentration (10%) would have a larger contribution from the flatter species, when compared to the saturated sample. The reason is that in the saturated sample the molecule lies in a tilted arrangement, which is not as effective in promoting the substituent twisting as the parallel one (low loading). Raman spectroscopy does not unequivocally support the hypothesis of substituent torsion, considering that aggregation is also happening. With the data available, it is not possible to differentiate the contributions from aggregation and from distortion; this point is currently under investigation and it will be reported soon.

4. Conclusions

The main interest in macrocycle immobilization is certainly associated with catalysis and biomimetic systems. In both cases, the effect of immobilization on the electronic structure and geometry of the guest molecule is of uppermost importance.

Concerning the porphyrins investigated here, two types of geometry change have to be considered: porphyrin ring distortion and rotation of the methylpyridyl group around the C_m—C_{MePy} bond. Since porphyrin ring distortion is accompanied by some degree of substituent twisting, it is not possible to separate their relative contributions. However, the data here reported for TMPyP and CoTMPyP conclusively shows that substituent torsion is not the most significant structural change promoted by the interaction with the clay.

The UV-VIS absorption spectra of TMPyP intercalated in the montmorillonites (K10 and KSF) and the fluorohectorite differ substantially from the pure porphyrin spectrum. The Soret and Q bands shift and broaden; their relative intensities are also affected by the interaction, which seems to cause a hypochromic effect in the Soret band. The same happens in the case of CoTMPyP, despite the smaller shifts and broadening.

Concerning TMPyP, it is difficult to state only from the UV-VIS data, whether or not macrocycle protonation is occurring upon interaction. In solution, it is easy to differentiate the free base from the diacid as the change in symmetry (from D_{2h} to D_{4h}) causes a change in the number of Q bands. For the intercalates studied here, the presence of both free base and protonated porphyrin, together with band broadening and shift, make it impossible to unequivocally identify the diacid features.

The Raman spectrum of the diprotonated porphyrin was obtained and compared with the intercalated ones. The good agreement among them combined with the X-ray diffraction data, clearly demonstrate that protonation is occurring to some extent in cases where the macrocycle lies in a flat arrangement relative to the clay layers (K10 and KSF). It is important to emphasize that the Raman and UV-VIS spectra have contributions from both protonated and non-protonated species.

The Raman spectra of the protonated TMPyP and of the intercalates present some discrepancies; at the moment it is not possible to ascertain whether they arise from ring distortions or from environment effects. This point is currently under investigation.

Acknowledgements

References

1. G. Lagaly and K. Beneke: *Colloid Polym. Sci*. **269**, 1198 (1991).
2. T. J. Pinnavaia: *Science* **220**, 365 (1983).
3. E. Kikuchi and T. Matsuda: *Catal. Today* **2**, 297 (1988).
4. A. Vaccari: *Catal. Today* **41**, 53 (1998).
5. C. J. B. Mott: *Catal. Today* **2**, 199 (1988).
6. L. R. Milgrom: *The Colours of Life – An Introduction to the Chemistry of Porphyrins and Related Compounds*, Oxford University Press, New York (1997).
7. N. Kaufherr, S. Yariv, and L. Heller: *Clays Clay Minerals* **19**, 193 (1971).
8. D. R. Kosiur: *Clays Clay Minerals* **25**, 365 (1977).
9. H. Van Damme, M. Crepin, F. Obrecht, M. I. Cruz, and J. J. Fripiat: *J. Colloid Interface Sci.* **66**, 43 (1978).
10. S. S. Cady and T. J. Pinnavaia: *Inorg. Chem.* **17**, 1501 (1978).
11. F. Bergaya and H. Van Damme: *Geochim. Cosmochim. Acta* **46**, 349 (1982).
12. K. A. Carrado and R. E. Winans: *Chem. Mater.* **2**, 328 (1990).
13. K. Sakoda and K. Kominami: *Chem. Phys. Lett.* **216**, 270 (1993).
14. H. Kaneyama, H. Suzuki, and A. Amabo: *Chem. Lett.* 1117 (1988).
15. E. P. Giannelis: *Chem. Mater.* **2**, 627 (1990).
16. L. Ukrainczyk, M. Chibwe, T. J. Pinnavaia, and S. A. Boyd: *J. Phys. Chem.* **98**, 2668 (1994).
17. K. A. Carrado, K. B. Anderson, and P. S. Grutkoski: in T. Bein (ed.), *Thermal Analysis of Porphyrin-Clay Complexes*, Supramolecular architecture – synthetic control in thin films and solids, ACS Symposium Series 499, pp. 155–165, American Chemical Society, Washington DC (1992).
18. K. A. Carrado and S. R. Wasserman: *Chem. Mater.* **8**, 219 (1996).
19. K. A. Carrado, P. Thiyagarajan, R. E. Winans, and R. E. Botto: *Inorg. Chem.* **30**, 794 (1991).
20. F. Bedioui: *Coord. Chem. Rev.* **144**, 39 (1995).

21. K. J. Balkus Jr. and A. G. Gabrielov: *J. Incl. Phenom. Mol. Rec. Chem.* **21**, 159 (1995).
22. L. Barloy, J. P. Lallier, P. Battioni, D. Mansuy, Y. Piffard, M. Tournoux, J. B. Valim, and W. Jones: *New J. Chem.* **16**, 71 (1992).
23. L. Ukrainczyk, M. Chibwe, T. J. Pinnavaia, and S. A. Boyd: *Environ. Sci. Technol.* **29**, 439 (1995).
24. M. Chibwe, L. Ukrainczyk, S. A. Boyd, and T. J. Pinnavaia: *J. Mol. Catal.* **113A**, 249 (1996).
25. A. C. Albrecht: *J. Chem. Phys.* **34**, 1476 (1961).
26. E. Unger, W. Dreybrodt, and R. Schweitzer-Stenner *J. Phys. Chem. A* **101**, 5997 (1997).
27. J. A. Shelnutt, C. J. Medforth, M. D. Berber, K. M. Barkigia, and K. M. Smith: *J. Am. Chem. Soc.* **113**, 4077 (1991).
28. J. Sun, C. K. Chang, and T. M. Loehr: *J. Phys. Chem. B* **101**, 1476 (1997).
29. C. M. Drain, S. Gentemann, J. A. Roberts, N. Y. Nelson, C. J. Medforth, S. Jia, M. C. Simpson, K. M. Smith, J. Fajer, J. A. Shelnutt, and D. Holten: *J. Am. Chem. Soc.* **120**, 3781 (1998).
30. D. S. Robins and P. K. Dutta: *Langmuir* **12**, 402 (1996).
31. B. Zhan and X. Li: *J. Chem. Soc. Chem. Commun.* 349 (1998).
32. M. A. Bizeto, D. L. A. de Faria, and V. R. L. Constantino: *J. Mater. Sci. Lett.* **18**, 643 (1999).
33. J. E. D. Davies: *J. Incl. Phenom. Mol. Recognit. Chem.* **24**, 133 (1996) and references therein.
34. M. J. Dickey and K. T. Carron: *Langmuir* **12**, 2226 (1996).
35. Y. Soma, M. Soma, and I. Harada: *J. Phys. Chem.* **88**, 3034 (1984).
36. Y. Soma, M. Soma, and I. Harada: *Chem Phys. Lett.* **94**, 475 (1983).
37. V. G. Kuykendall and J. K. Thomas: *Langmuir* **6**, 1350 (1990).
38. Z. Chernia and D. Gill: *Langmuir* **15**, 1625 (1999).
39. N. Blom, J. Odo, and K. Nakamoto: *J. Phys. Chem.* **90**, 2847 (1986).
40. R. Schweitzerstenner, A. Stichternath, W. Dreybrodt, W. Jentzen, X. Z. Song, J. A. Shelnutt, O. F. Nielsen, C. J. Medforth, and K. M. Smith: *J. Chem. Phys.* **107**, 1794 (1997).
41. K. Prendergast and T. G. Spiro: *J. Am. Chem. Soc.* **114**, 3793 (1992).
42. C. Lemke, W. Dreybrodt, J. A. Shelnutt, J. M. E. Quirke, and R. Schweitzer-Stenner: *J. Raman Spectrosc..* **29**, 945 (1998).
43. J. Chaussidon, R. Calvet, J. Helsen, and J. J. Fripiat: *Nature* **196**, 161 (1962).
44. G. M. Williams, J. Olmsted III, and A. P. Breksa III: *J. Chem. Educ.* **66**, 1043 (1989).
45. J.-R. Brutuille and T. J. Pinnavaia: *Catal. Today* **14**, 141 (1992).
46. M. Onaka, T. Shinoda, Y. Izumi, and E. Nolen: *Chem. Lett.* 117 (1993).
47. G. W. Brindley and G. Brown (eds.): *Crystal Structures of Clay Minerals and their X-ray Identification*, Mineralogical Society, London (1984).
48. T. Nakato, Y. Iwata, K. Kuroda, M. Kaneko, and C. Kato: *J. Chem. Soc. Dalton Trans.* 1405 (1993).
49. M. Gouterman: The porphyrins, in D. Dolphin (ed.), *Optical Spectra and Electronic Structure of Porphyrins and Related Rings*, Vol. 2, Academic Press, New York (1979).
50. I. Y. Chan and A. J. Hallock: *J. Chem. Phys.* **107**, 9297 (1997).
51. C. T. Johnston: Organic pollutants in the environment, in B. L. Sawhney (ed.), *Sorption of Organic Compounds on Clay Minerals: A Surface Functional Group Approach*, Vol. 8, CMS Workshop Lectures, The Clay Minerals Society, Boulder (1996).
52. R. F. Pasternack, N. Sutin, and D. H. Turner: *J. Am. Chem. Soc.* **98**, 1908 (1976).
53. A. Stone and E. B. Fleischer: *J. Am. Chem. Soc.* **90**, 2735 (1968).